

Time-resolved soft x-ray absorption setup using multi-bunch operation modes at synchrotrons

L. Stebel, M. Malvestuto, V. Capogrosso, P. Sigalotti, B. Ressel et al.

Citation: *Rev. Sci. Instrum.* **82**, 123109 (2011); doi: 10.1063/1.3669787

View online: <http://dx.doi.org/10.1063/1.3669787>

View Table of Contents: <http://rsi.aip.org/resource/1/RSINAK/v82/i12>

Published by the [American Institute of Physics](#).

Related Articles

Transport mechanism of MeV protons in tapered glass capillaries

J. Appl. Phys. **110**, 044913 (2011)

Generation of multi-color attosecond x-ray radiation through modulation compression

Appl. Phys. Lett. **99**, 081101 (2011)

Compact and high-quality gamma-ray source applied to 10 m-range resolution radiography

Appl. Phys. Lett. **98**, 264101 (2011)

A Mott polarimeter operating at MeV electron beam energies

Rev. Sci. Instrum. **82**, 033303 (2011)

Wake potentials and impedances of charged beams in gradually tapering structures

J. Math. Phys. **52**, 032902 (2011)

Additional information on Rev. Sci. Instrum.

Journal Homepage: <http://rsi.aip.org>

Journal Information: http://rsi.aip.org/about/about_the_journal

Top downloads: http://rsi.aip.org/features/most_downloaded

Information for Authors: <http://rsi.aip.org/authors>

ADVERTISEMENT

**AIP**Advances

Submit Now

**Explore AIP's new
open-access journal**

- **Article-level metrics
now available**
- **Join the conversation!
Rate & comment on articles**

Time-resolved soft x-ray absorption setup using multi-bunch operation modes at synchrotrons

L. Stebel,¹ M. Malvestuto,^{1,2,a)} V. Capogrosso,^{1,2} P. Sigalotti,¹ B. Ressel,¹ F. Bondino,³ E. Magnano,³ G. Cautero,¹ and F. Parmigiani^{1,2,3}

¹*Sincrotrone Trieste, S.S. 14 km 163.5, Area Science Park, 34149 Basovizza (Ts), Italy*

²*Department of Physics, University of Trieste, via A. Valerio 2, 34127, Trieste, Italy*

³*IOM-CNR, TASC laboratory, S.S. 14 km 163.5, Area Science Park, 34149 Basovizza (Ts), Italy*

(Received 26 August 2011; accepted 27 November 2011; published online 16 December 2011)

Here, we report on a novel experimental apparatus for performing time-resolved soft x-ray absorption spectroscopy in the sub-ns time scale using non-hybrid multi-bunch mode synchrotron radiation. The present setup is based on a variable repetition rate Ti:sapphire laser (pump pulse) synchronized with the ~ 500 MHz x-ray synchrotron radiation bunches and on a detection system that discriminates and singles out the significant x-ray photon pulses by means of a custom made photon counting unit. The whole setup has been validated by measuring the time evolution of the L_3 absorption edge during the melting and the solidification of a Ge single crystal irradiated by an intense ultrafast laser pulse. These results pave the way for performing synchrotron time-resolved experiments in the sub-ns time domain with variable repetition rate exploiting the full flux of the synchrotron radiation. © 2011 American Institute of Physics. [doi:10.1063/1.3669787]

I. INTRODUCTION

The x-ray absorption spectroscopy (XAS) is a widely used and well-established method for studying the electronic states and the local magnetic properties of matter at equilibrium. Adding the time-domain to XAS spectroscopy, the excited and transient states of complex systems become directly observable.

As a whole, free electron lasers and synchrotron slicing sources are suitable for time-resolved experiments in time domains of tens of fs or less. Otherwise utilizing the time structure of the synchrotron sources, time-resolved XAS (TR-XAS) experiments are accessible with a time resolution which is limited by the length of the electron bunches, i.e., typically a few tens of ps. While most users exploit synchrotron radiation (SR) in multi-bunch filling mode as a very intense quasi-continuous light source, conventional laser-pump SR-probe experiments require the storage ring operating with dedicated filling modes, e.g., single-bunch, few-bunches, and hybrid modes.^{1–22} To overcome this limitation and to operate at variable repetition rates, the use of the multi-bunch filling pattern must be implemented with novel and effective acquisition concepts and ideas to perform time-resolved experiments in the sub-ns time domain.²³

Scope of this work is to report on a synchronized laser-pump SR-probe apparatus suitable for sub-nanosecond TR-XAS enhanced pump-probe experiments on conventional third generation storage rings. In the specific, the improvements obtained with the present setup are displayed in Figure 1.

In a conventional laser-pump x-ray-probe experiment, a laser pulse excites a transient state while a x-ray pulse, at a fixed delay time relative to the laser pulse, probes the non-equilibrium states. Here, the synchrotron x-ray pulses, fol-

lowing in time the laser excitation, are used to probe the relaxation process of the excited states allowing to observe the complete dynamical evolution at once. Moreover, the photon counting approach, adopted to measure the x-ray fluorescence emission fully exploits the available x-ray photon flux at ~ 500 MHz repetition rate as a stroboscopic probing sequence thus providing continuous snapshots of the transient state spectra. For sake of clarity a simplified schematic of the acquisition flow is shown in Figure 2.

Lastly, for endorsing the effectiveness and reliability of this novel pump-probe technique, the melting and solidification dynamics of a Ge single crystal induced by femtosecond-laser pulses is reported. The comparison of TR-XAS data with time-resolved conductivity measurements²⁴ fully validates the present setup for sub-ns time-resolved XAS experiments.

II. EXPERIMENTAL SETUP

The time-resolved XAS setup is operating at the end-station B of the BACH beamline at Elettra.^{25,26} A wide range of experimental conditions can be accomplished, thanks to a high intensity photon beam ($\sim 10^{12}$ photons/s) in the soft x-rays energy range (46–1600 eV) with control over light polarization (linear vertical, linear horizontal, circular clockwise and counterclockwise).

The Elettra storage ring, in its standard operating mode, delivers x-ray pulses with low intensity (e.g., 10^2 – 10^3 photons/pulse in a monochromatic beam at ID8.1) and a high repetition rate. Typically, the filling mode is multi-bunch, i.e., 432 electron bunches with ~ 60 ps full-width-half-maximum (FWHM) rotating in the storage ring with ~ 2 ns inter-bunch period and a resulting 1.157 MHz revolution frequency. A dark gap is present, consisting of about 30 electron bunches

^{a)}Electronic mail: marco.malvestuto@elettra.trieste.it.

Conventional pump-probe (e.g. with few bunch mode)

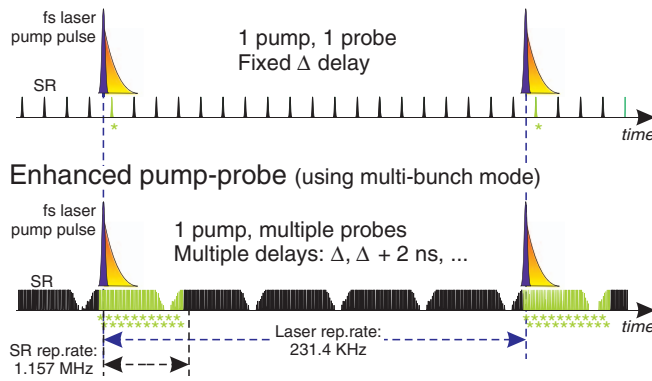


FIG. 1. (Color online) Comparison between conventional pump-probe and the present enhanced pump-probe scheme, which exploits the high repetition rate of the multi-bunch filling mode of the synchrotron source. In the conventional pump-probe experiment (top), a single x-ray pulse cyclically probes the transient state at the laser repetition rate (~ 250 kHz) and at fixed delay time Δ relative to the laser pulse. In the enhanced pump multiple-probe scheme (bottom), a train of consecutive x-ray pulses at ~ 500 MHz repetition rate and synchronized with the laser pulse, probes the transient state at multiple delays (Δ ns, $\Delta + 2$ ns, ...) for its entire lifetime.

with a very reduced amplitude. The main timing parameters of the Elettra light source are reported in Table I.

The samples are positioned in an ultrahigh vacuum chamber and mounted on a suitable motor-controlled manipulator. The laser beam enters the experimental chamber through a quartz window at an angle of 30° with respect to the x-ray photon beam. The x-ray fluorescence emission is detected by

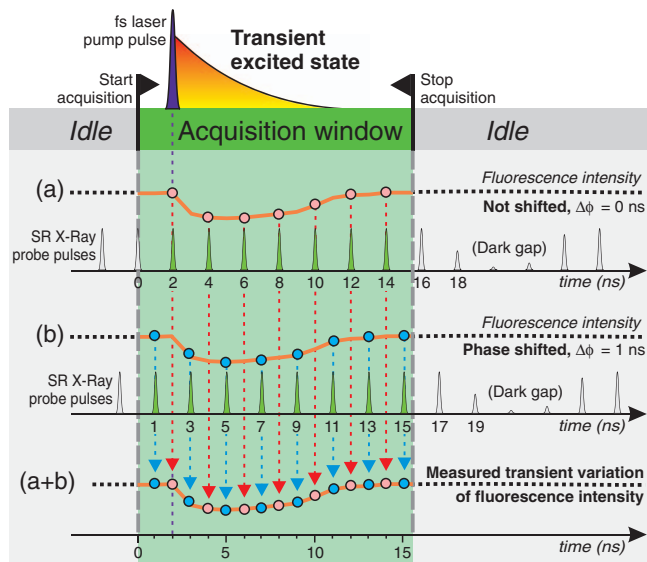


FIG. 2. (Color online) (a) The transient state is sampled during a well-defined acquisition window (green interval) that is repeated iteratively at the repetition rate of the laser source. The acquisition window selects a number of consecutive x-ray probing pulses. Usually, the photon dark gap is used as a reference to check the acquisition status and to measure the noise signal from the x-ray photon detector. (b) In order to map out the temporal behavior of the transient state with a time sampling step lower than 2 ns, phase shifted acquisitions with different pump-probe time alignment are performed. The photon bunches before the laser pulse arrival ($t = 0$), probing the XAS spectrum of the non-excited state, are used as a reference.

TABLE I. Timing parameters of the Elettra storage ring.

Parameter	Value
Accelerating frequency (RF)	499.65 MHz
Number of electron bunches	432
Revolution frequency	1.157 MHz
Typical bunch width	~ 60 ps

an ultrafast micro-channel plate (MCP) x-ray detector set at 60° off the incoming x-ray photon beam.

The amplified laser source operates at variable repetition rate (230 kHz–83.3 MHz) and delivers ~ 5 μ J to ~ 25 nJ, ~ 100 fs, 800 nm laser pulses. The fundamental wavelength can be converted into 400 nm light by second harmonic generation (Table II). The laser is focused on the sample by a fixed 50 mm focusing lens, while the focus size is adjusted operating on the sample position.

The pump laser pulses are accurately synchronized to the x-ray probe arrays so that the relative time delay is maintained equal for all data acquisition windows. The pump (laser)-probe (x-ray) sources synchronization is achieved by exploiting the radio frequency (RF) master clock of Elettra that provides the time structure of the generated radiation. The RF is divided by a timing unit that also allows for the remote control of the relative time delay by phase shifting the oscillator frequency with respect to the master RF. The phase stabilization of the laser source is achieved via a synchronization unit, which locks the laser oscillators to the Elettra master RF with a time jitter < 2 ps.

III. THE DETECTION AND ACQUISITION SYSTEMS

The data collection approach consists in counting the x-ray fluorescence emission. Being the lifetimes of the excited core holes of the order of few fs, the time structures of the x-ray fluorescence emission and of the x-ray-probe array coincide. For this reason, the measured FY signal is a temporally undistorted probe of the dynamical properties of the transient states. In addition, since the x-ray fluorescence photons are rare events if compared to the non-radiative de-excitations, the FY signal does not saturate the electronic response of the photon detector. The overall detection rate is thus dictated by the maximum dynamical range of the detector (5×10^6 counts/s or 0.04 photons/bunch), while the high x-ray photon flux still guarantees a very high counting statistics (number of detected photons per second). The combination of this acquisition strategy with an ultrafast MCP detector (rise time

TABLE II. Timing parameters of the Ti:Sa laser source.

	RegA9000	Mira HP
Wavelength	800 nm; SHG: 400 nm	800 nm; SHG: 400 nm
Pulse width	100 fs	100 fs
Pulse energy	5 μ J/pulse	25 nJ/pulse
Repetition rate	200–250 kHz	variable [5–0.01 MHz] 83.3 MHz

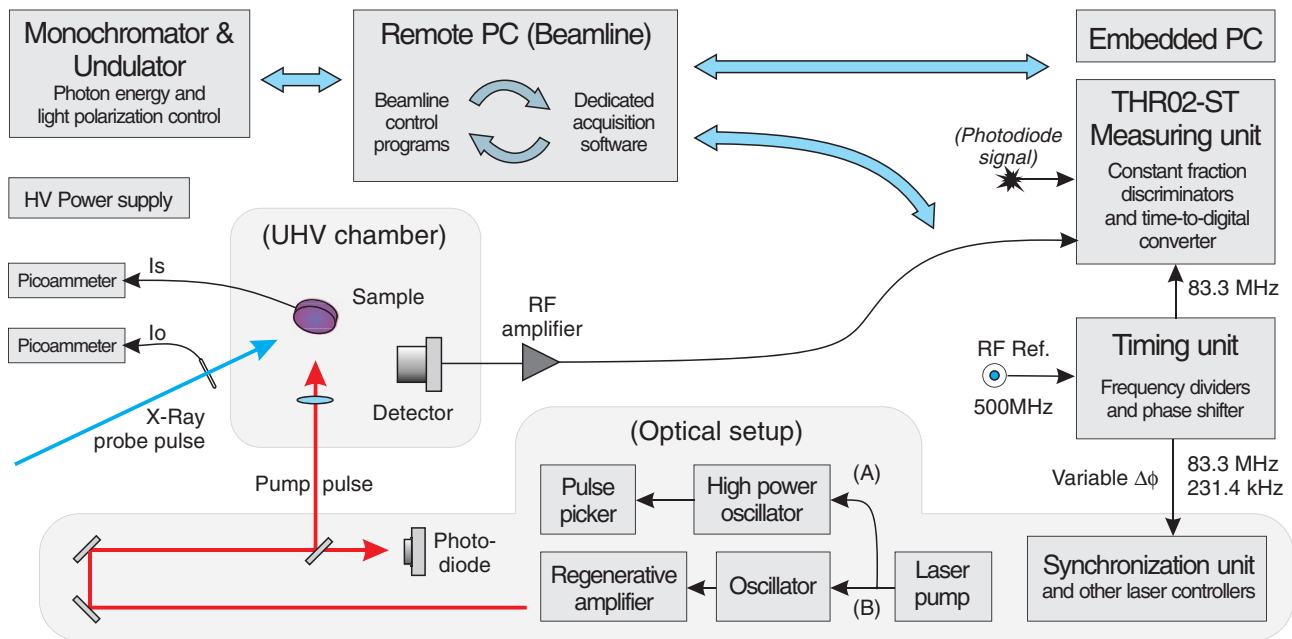


FIG. 3. (Color online) Schematic layout of the experimental setup for a pump-probe XAS measurement, with its three main sections: the beamline environment (UHV chamber, picoammeters, power supplies, undulator, monochromator, and remote PC), the optical setup (laser sources and controllers), and the measuring setup (THR02-ST measuring unit, timing unit and embedded PC).

~ 300 ps (Ref. 27)) results in an acquisition system that is fast enough to isolate the x-ray pulses coming from each consecutive photon bunch and still maintaining a linear response over the entire x-ray flux range.

A scheme of the detection and acquisition system is shown in Figure 3. The custom made THR02-ST (Ref. 28) measuring device and the timing unit are the main components of the whole detection apparatus. The embedded PC is used for monitoring the system while acting as a communication bridge between the remote PC and the measuring setup.

The THR02-ST measuring unit is based on a time-to-digital converter (TDC) controlled by a field programmable gate array (FPGA) that allows the interactive control of the acquisition parameters.

After a trigger signal is asserted, the measuring unit starts recording the arrival time of all the detected events occurring during a configurable acquisition time window (typically 864 ns corresponding to a complete synchrotron revolution period). The MCP analog output signal is amplified, shaped, and widened to about 4 ns so that the signal can be digitized using a constant fraction discriminator (CFD) which selects the centroid of the pulse discarding the effects of signal amplitude variations. The CFD output is finally recorded by the THR02-ST unit. Typical acquisition time histograms as a function of photon bunches and photon energy are shown in the main panel of Figure 4. The acquisition windows are cyclically activated at the laser repetition rate until significant statistics is achieved. The resulting unit time of the acquisition system is equal to the bin size of the TDC (~ 27 ps), while the final time resolution is the FWHM of the Gaussian peak in a counts vs time histogram (see inset in Figure 4) measured under bench test conditions.

The timing unit includes two fully configurable frequency dividers and a phase shifter unit based on I/Q mod-

ulation. Starting from the ~ 500 MHz RF master clock of the storage ring, by means of the frequency dividers, the proper reference signals are generated for the laser setup, locking the laser at a 231.4 kHz repetition rate with a stable and editable phase delay relative to the selected electron bunch. A non-phase shifted 83.3 MHz signal makes the FPGA synchronous with the acquisition system allowing the measuring unit to trigger the acquisition windows while maintaining a constant phase relationship with the synchrotron bunch train. The

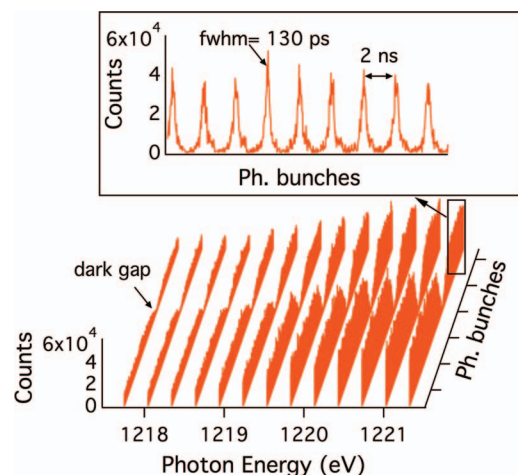


FIG. 4. (Color online) Typical acquisition time histograms (counts vs consecutive photon bunches), taken at different x-ray photon energies through an absorption threshold (in this example, the Ge L_3 threshold). The constant time position of the dark gap indicates the overall stability of the synchronization between the probe and pump sources. Inset: pulse height distribution of consecutive x-ray photon bunches recorded at fixed energy and without laser. The x-ray fluorescence signal clearly inherits the time structure of the storage ring filling pattern (2 ns time separation between two consecutive photon pulses), while the standard deviation (FWHM = 130 ps) of each measured pulse is wider than the typical width of electron bunches (60 ps).

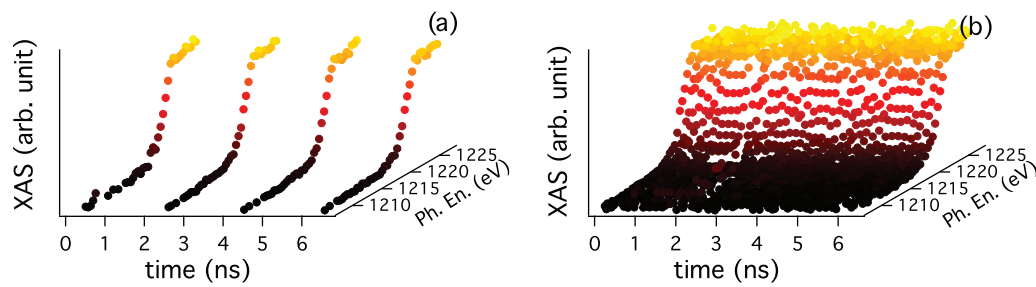


FIG. 5. (Color online) Comparison between a standard multi-probe TR-XAS spectra (a) and a denser phase scan spectra (b). Figure 5(a) shows four consecutive Ge L_3 TR-XAS spectra separated by 2 ns inter-bunch delay. The intensity of each XAS point is obtained by integrating a single photon bunch (i.e., histogram peak, see inset of Figure 4) per time and per energy step. Figure 5(b) shows a phase scan, i.e., consecutive XAS spectra obtained in the same operating conditions of Figure 5(a) but with incremental 100 ps laser-SR delay shifts.

timing unit can be used to perform phase shifted TR-XAS spectra, with 100 ps or even smaller steps, i.e., with a time-base comparable to the overall time resolution, as illustrated in Figures 5(a) and 5(b).

Another challenging aspect for performing laser-pump x-ray-probe experiments is given by the spatial and temporal overlap of the two light beams. In the present experiment, the spatial alignment is made by using a phosphor screen positioned in place of the sample. The $\sim 50 \mu\text{m}$ x-ray spot and the $\sim 50 \mu\text{m}$ laser spot are then superimposed by using a CCD camera and by moving the laser beam position until a satisfactory spatial overlap is achieved. For the temporal overlap, the attenuated second harmonic of the pump laser scattered from the sample is detected by the MCP and singled out in the counts versus time histogram. From this picture the relative time delay between the pump and probe sources can be directly observed and adjusted by acting on the phase shifter in the timing unit.

IV. EXPERIMENTAL RESULTS

Time-resolved XAS can be used as a novel spectroscopy in the time domain for studying transient states of high temperature materials and photoinduced phase transitions produced by intense optical pulses.^{29–35} As a proof of principle for the present TR-XAS setup, herewith below we report on time-resolved XAS spectra of the laser induced solid-liquid-solid transitions of crystalline Ge.³⁶ This semiconductor is of particular interest for testing our setup for its absorption edges in the liquid phase are shifted about 0.7 eV towards lower photon energies (cf. Ge K_α (Ref. 37) and $M_{2,3}$ (Refs. 38, 39) edges), while the liquid-solid phase transition is expected to take place on a time scale of few ns.²⁴ The XAS spectra have been taken at the Ge L_3 edge. A representative selection of such spectra is shown in Figure 5. The XAS spectra are plotted versus the time delay and versus the x-ray photon energy. The origin of the time scale is set accordingly to the pump pulse arrival time. The acquisition lasts 20 s per energy point and 30 min for completing a suitable time-resolved spectra. The XAS spectra of the Ge, recorded under pump-probe conditions at a laser fluence below the Ge surface-melting critical fluence, i.e., 110 mJ/cm², are shown in Figure 5 for a fixed pump-to-probe delay time (Figure 5(a)) and for a varied delay time (Figure 5(b)). As expected these spectra exhibit the

typical solid Ge L_3 lineshape (cf. Ref. 40) for each temporal snapshot after the absorption of the laser pulse. The full set of spectra recorded with the laser pump fluence below threshold, i.e., 110 mJ/cm², at photon probe energies between 1216 eV and 1224 eV and for time delays between 0 ns and 300 ns is reported in Figure 6(a). The uniformity of the color indicates that all the spectra are identical, reflecting the fact that the surface is still a solid.

A typical example of TR-XAS spectra, as measured with the present setup while the sample is undergoing solid-liquid phase transitions, is reported in Figure 6(b). The spectra

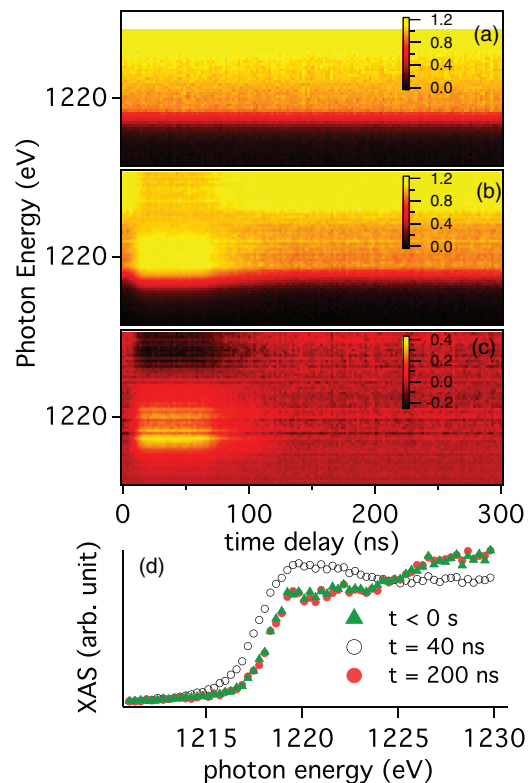


FIG. 6. (Color online) Intensity plots of L_3 TR-XAS spectra of a not-melted (a) and melted (b) Ge sample. The XAS spectra intensities are plotted versus the photon bunch arrival time (the laser pulse: $t = 0$) and versus the x-ray photon energy. Figure 6(c): difference map obtained as the difference between the TR-XAS spectra in Figure 6(b) and a ground state XAS spectrum measured at $t < 0$. Figure 6(d): Ge L_3 TR-XAS lineshapes sliced from the intensity plot in (b) and taken at different time delays with respect to the laser pulse.

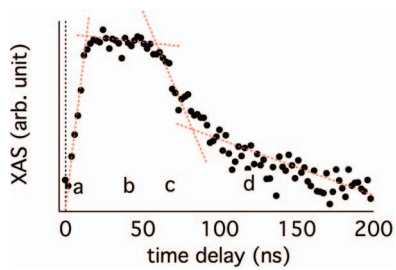


FIG. 7. (Color online) This figure shows a slice at constant photon energy (1219.0 eV) of the intensity plot shown in Figure 6(b). This TR-XAS relative intensity variation as a function of time can be divided into four regions (a, b, c, and d) according to its slope (see text).

reported in Figures 6(b)–6(d) have been obtained using a laser fluence of 120 mJ/cm². This set of data shows, in false colors, the dynamics of the melting as measured from the Ge L_3 absorption edge for a photon energy range between 1216 eV and 1224 eV and for pump-probe delay times between 0 ns and 300 ns. Figure 6(d) reports the TR-XAS spectra at constant delay times ($t < 0$, $t = 40$ ns, and $t = 200$ ns), quite representative of the solid-liquid-solid phase transition dynamics of a Ge crystal. The TR-XAS spectra present dramatic changes of the lineshapes and absorption edge energy position as a function of the pump-probe delay time. The onset of the Ge L_3 absorption edge at a delay time of about 10 ns is shifted by $\sim 0.7 \pm 0.1$ eV with respect to the solid Ge edge, as shown in Figure 6(c). The magnitude of the absorption edge is increased by $\sim 30\%$ and the small fine structure at 1229 eV disappears (cf. Ref. 37).

Indeed, the relative XAS intensity variation reported in Figure 7 as a function of time can be divided into four regions. In region *a*, the solid Ge underneath the area illuminated by the laser starts melting and, consequently, the solid-liquid front propagates into the probed volume. In region *b*, the liquid cools down by conduction into the surrounding solid. The nucleation of the supercooled liquid is in part *c*, while in region *d* the solidification process occurs at constant rate.

Notably, the laser induced solid-liquid-solid dynamic melting of Ge, as resulting from the present experiment, is fully consistent with that obtained by Stiffler *et al.*²⁴ using time-resolved conductivity measurements. However, an extensive discussion about the solid-liquid-solid laser induced phase transition of Ge crystals overtakes the scope of the present work and it will be discussed in details elsewhere. Nonetheless, this comparison endorses completely the reliability of the laser-synchrotron pump-probe technique described in this work. In the meantime, the possibility of performing pump-multiple-probe experiments in the 100 ps time scale with variable repetition rate while operating the storage ring in multi-bunch mode, unlocks the gate for a huge variety of time-resolved experiments based on synchrotron conventional spectroscopies and scattering techniques.

V. CONCLUSIONS AND FUTURE OUTLOOK

Here, we have reported on the design, construction, and commissioning of an apparatus suitable for laser-pump SR-

probe time-resolved measurements in the sub-ns time domain. The system operates by exploiting the multi-bunch filling mode of the Elettra synchrotron storage ring to probe the optically excited state with a continuous array of x-ray pulses. Thus, the unique time structure of the x-ray synchrotron pulses allows to take snapshots of the transient excited state at consecutive and increasing delay times.

By exploiting this setup, we have proved the feasibility of measuring, with a time resolution of about 100 ps, the transient changes of the structurally relevant $2p - 4s$ (L_3) XAS spectra during the solid-liquid-solid phase transition of a crystalline Ge sample irradiated by an ultrashort laser pulse.

The development of a TR-XAS technique at the BACH beamline or at similar beamlines, with a ~ 100 ps time resolution and the possibility of exploiting the 500 MHz multi-bunch filling pattern of the storage ring, opens the route to several new experiments in the sub-ns time domain using synchrotron light.

ACKNOWLEDGMENTS

We acknowledge the precious support from the Laboratory for time-resolved Experiments at Elettra, the Detectors and Instrumentations Laboratory, and the BACH beamline staff. M.M. is grateful to Federico Salvador for technical support and to Dr. Federico Cilento for fruitful discussions. F.P. acknowledges partial financial support by MIUR-PRIN 2008 project.

- ¹A. March, A. Stickrath, G. Doumy, E. Kanter, B. Krassig, S. Southworth, K. Attenkofer, C. Kurtz, L. Chen, and L. Young, *Rev. Sci. Instrum.* **82**, 073110 (2011).
- ²W. Gawelda, V. Pham, M. Benfatto, Y. Zaushitsyn, M. Kaiser, D. Grolimund, S. Johnson, R. Abela, A. Hauser, and C. Bressler, *Phys. Rev. Lett.* **98**, 57401 (2007).
- ³W. Gawelda, M. Johnson, F. de Groot, R. Abela, C. Bressler, and M. Chergui, *J. Am. Chem. Soc.* **128**, 5001 (2006).
- ⁴W. Gawelda, C. Bressler, M. Saes, M. Kaiser, A. Tarnovsky, D. Grolimund, S. Johnson, R. Abela, and M. Chergui, *Phys. Scr.*, **T 115**, 102 (2005).
- ⁵M. Saes, F. Van Mourik, W. Gawelda, M. Kaiser, M. Chergui, C. Bressler, D. Grolimund, R. Abela, T. Glover, and P. Heimann, *Rev. Sci. Instrum.* **75**, 24 (2004).
- ⁶C. Bressler and M. Chergui, *Chem. Rev.* **104**, 1781 (2004).
- ⁷C. Bressler, M. Saes, M. Chergui, R. Abela, and P. Pattison, *Nucl. Instrum. Methods Phys. Res., A* **467-468**, 1444 (2001).
- ⁸C. Bressler, M. Saes, M. Chergui, D. Grolimund, R. Abela, and P. Pattison, *J. Chem. Phys.* **116**, 2955 (2002).
- ⁹M. Saes, C. Bressler, R. Abela, D. Grolimund, S. Johnson, P. Heimann, and M. Chergui, *Phys. Rev. Lett.* **90**, 474031 (2003).
- ¹⁰L. Chen, *Angew. Chem., Int. Ed.* **43**, 2886 (2004).
- ¹¹E. Dufresne, B. Adams, M. Chollet, R. Harder, Y. Li, H. Wen, S. Leake, L. Beitra, X. Huang, and I. Robinson, *Nucl. Instrum. Methods Phys. Res. A* **649**, 191 (2011).
- ¹²T. Matsunaga, J. Akola, S. Kohara, T. Honma, K. Kobayashi, E. Ikenaga, R. Jones, N. Yamada, M. Takata, and R. Kojima, *Nature Mater.* **10**, 129 (2011).
- ¹³T. Gießel, D. Bröcker, P. Schmidt, and W. Widdra, *Rev. Sci. Instrum.* **74**, 4620 (2003).
- ¹⁴J. Labiche, O. Mathon, S. Pascarelli, M. Newton, G. Ferre, C. Curfs, G. Vaughan, A. Homs, and D. Carreiras, *Rev. Sci. Instrum.* **78**, 091301 (2007).
- ¹⁵A. Lindenberg, I. Kang, S. Johnson, T. Missalla, P. Heimann, Z. Chang, J. Larsson, P. Bucksbaum, H. Kapteyn, and H. Padmore, *Phys. Rev. Lett.* **84**, 111 (2000).
- ¹⁶J. Larsson, P. A. Heimann, A. M. Lindenberg, P. J. Schuck, P. H. Bucksbaum, R. W. Lee, H. A. Padmore, J. S. Wark, and R. W. Falcone, *Appl. Phys. A* **66**, 587 (1998).

- ¹⁷C. Rischel, A. Rousse, I. Uschmann, P. Albouy, J. Geindre, P. Audebert, J. Gauthier, E. Fröster, J. Martin, and A. Antonetti, *Nature (London)* **390**, 490 (1997).
- ¹⁸C. P. Barty, F. Raksi, C. G. Rose-Petruck, K. J. Schafer, K. R. Wilson, V. V. Yakovlev, K. Yamakawa, Z. Jiang, A. Ikhlef, C. Y. Cote, and J.-C. Kieffer, *Proc. SPIE* **2521**, 246 (1995).
- ¹⁹V. Petkov, S. Takeda, Y. Waseda, and K. Sugiyama, *J. Non-Cryst. Solids* **168**, 97 (1994).
- ²⁰T. Anderson, I. Tomov, and P. Rentzepis, *J. Chem. Phys.* **99**, 869 (1993).
- ²¹H. Ichikawa, S. Nozawa, T. Sato, A. Tomita, K. Ichiyangi, M. Chollet, L. Guerin, N. Dean, A. Cavalleri, S.-I. Adachi, T.-H. Arima, H. Sawa, Y. Ogimoto, M. Nakamura, R. Tamaki, K. Miyano, and S.-Y. Koshihara, *Nature Mater.* **10**, 101 (2011).
- ²²F. Lima, C. Milne, D. Amarasinghe, M. Rittmann-Frank, R. Veen, M. Reinhard, V.-T. Pham, S. Karlsson, S. Johnson, D. Grolimund, C. Borca, T. Huthwelker, M. Janousch, F. Van Mourik, R. Abela, and M. Chergui, *Rev. Sci. Instrum.* **82**, 063111 (2011).
- ²³N. Bergeard, M. Silly, D. Krizmanic, C. Chauvet, M. Guzzo, J. Ricaud, M. Izquierdo, L. Stebel, P. Pittana, R. Sergo, G. Cautero, G. Dufour, F. Rochet, and F. Sirotti, *Synchrotron Radiat.* **18**, 245 (2011).
- ²⁴S. Stiffler, M. Thompson, and P. Percy, *Appl. Phys. Lett.* **56**, 1025 (1990).
- ²⁵M. Zangrando, M. Zacchigna, M. Finazzi, D. Cocco, R. Rochow, and F. Parmigiani, *Rev. Sci. Instrum.* **75**, 31 (2004).
- ²⁶M. Zangrando, M. Finazzi, G. Paolucci, G. Comelli, B. Diviacco, R. P. Walker, D. Cocco, and F. Parmigiani, *Rev. Sci. Instrum.* **72**, 1313 (2001).
- ²⁷See www.hamamatsu.com for Hamamatsu Photonics.
- ²⁸See <http://www.elettra.trieste.it/ilo>.
- ²⁹J. Workman, M. Nantel, A. Maksimchuk, and D. Umstadter, *Appl. Phys. Lett.* **70**, 312 (1997).
- ³⁰F. Ráksi, K. Wilson, Z. Jiang, A. Ikhlef, C. Côté, and J.-C. Kieffer, *J. Chem. Phys.* **104**, 6066 (1996).
- ³¹F. Raksi, K. R. Wilson, Z. Jiang, A. Ikhlef, C. Y. Cote, and J.-C. Kieffer, *Proc. SPIE* **2523**, 306 (1995).
- ³²Y. Okano, K. Oguri, T. Nishikawa, and H. Nakano, *Rev. Sci. Instrum.* **77**, 046105 (2006).
- ³³K. Oguri, Y. Okano, T. Nishikawa, and H. Nakano, *AIP Conf. Proc.* **1278**, 656 (2010).
- ³⁴H. Nakano, K. Oguri, Y. Okano, and T. Nishikawa, *Proc. SPIE* **6614**, 661409 (2007).
- ³⁵H. Nakano, Y. Goto, P. Lu, T. Nishikawa, and N. Uesugi, *Appl. Phys. Lett.* **75**, 2350 (1999).
- ³⁶E. Stern, D. Brewes, K. Beck, S. Heald, and Y. Feng, *Phys. Scr., T* **T115**, 1044 (2005).
- ³⁷A. Filipponi, V. Giordano, and M. Malvestuto, *Phys. Status Solidi B* **234**, 496 (2002).
- ³⁸A. Goldoni, A. Santoni, M. Sancrotti, V. Dhanak, and S. Modesti, *Surf. Sci.* **382**, 336 (1997).
- ³⁹A. Di Cicco, B. Giovenali, R. Gunnella, E. Principi, and S. Simonucci, *Solid State Commun.* **134**, 577 (2005).
- ⁴⁰P. Castrucci, R. Gunnella, M. De Crescenzi, M. Sacchi, G. Dufour, and F. Rochet, *Phys. Rev. B* **60**, 5759 (1999).